Accumulation of Solar Irradiance Anomaly as a Mechanism for Global Temperature Dynamics

David R.B. Stockwell*

August 9, 2011

Abstract

Global temperature (GT) changes over the 20th century and glacial-interglacial periods are commonly thought to be dominated by feedbacks, with relatively small direct effects from variation of solar insolation. Here is presented a novel empirical and physically-based auto-regressive AR(1) model, where temperature response is the integral of the magnitude of solar forcing over its duration, and amplification increases with depth in the atmospheric/ocean system. The model explains 76% of the variation in GT from the 1950s by solar heating at a rate of $0.06 \pm 0.03 KW^{-1}m^{-2}Yr^{-1}$ relative to the solar constant of $1366 Wm^{-2}$. Miss-specification of long-equilibrium dynamics by empirical fitting methods (as shown by poor performance on simulated time series) and atmospheric forcing assumptions have likely resulted in underestimation of solar influence. The solar accumulation model is proposed as a credible mechanism for explaining both paleoclimatic temperature variability and present-day warming through high sensitivity to solar irradiance anomaly.

1 Introduction

The solar contribution to global warming since the mid-20th century is not settled (e.g. [1], vs. [2]). The flat warming/cooling rate of $0.1 \pm 0.2 W/m^2$ ocean heat content anomaly has not been

*davids99us@gmail.com

reconciled with the computed large, positive radiative imbalance of $0.6 \pm 0.3W/m^2$ ([3] and [4]). Climate models exhibit a tropical, upper tropospheric 'hotspot' that has not yet been observed [5, 6].

Examples of this sort suggest, contrary to conventional views [7], that factors may be missing that are critical to system understanding. Here we describe physics-based and empirical support for the resolution of these and other difficulties via accumulation of solar irradiation anomaly. The total variation in solar irradiation (TSI) available to influence GT directly is extremely low. For example, TSI at the surface varies by about $0.2W/m^2$ over the 11 year solar cycle, by $0.3W/m^2$ last century [8] and $0.5W/m^2$ over 100,000 year orbital variations [9]. These small changes in flux would immediately alter the temperature of a black body less than 0.1K using the linear Plank response of $0.3K/W/m^2$. Accumulation of heat from $0.1W/m^2$ for a one year, however, would move $3.1x10^6$ Joules of heat ($31x10^6$ sec/Yr) to the ocean, heating the mixed zone to 150m by about 0.006K (4.2 J/gK), producing the observed GT increase of 0.6K in 100 years and a glacial/interglacial transition in 1000 years.

2 Models

Consider the Sun at equilibrium with the Earth's surface. An increase in the shortwave radiation ΔS will cause mass C to accumulate heat and increase temperature ΔT. The temperature stops increasing when the outgoing longwave radiation ΔL equals ΔS, determined by $\lambda \Delta L = \Delta T$ where λ is in units of Kelvin per Watt per meter squared (K/Wm^2). The Earth will lose heat in a controlled fashion, proportional to the extra T over the equilibrium. In this basic energy balance model (EBM), small lambda means fast and direct relations to the forcing; large lambda means large, slow increases to equilibrium related by a ordinary differential equation [10]:

$$C\frac{dT}{dt} = S - \frac{T}{\lambda} \tag{1}$$

The discrete form of Eqn. 1 is a first order autoregressive AR(1) model:

$$T_t = (1 - \frac{1}{C\lambda})T_{t-1} + \frac{S_{t-1}}{C} + \epsilon \tag{2}$$

The AR recurrence model has physical meaning: $a = 1 - \frac{1}{C\lambda}$ is the fractional accumulation of heat at each time step and $1 - a$ is the fractional loss or leakage. Tau, $\tau = \frac{1}{1-a}$ is both the characteristic decay time and the system gain, that with the dilution of heat (and so temperature) by the mass C determines sensitivity to a forcing at equilibrium (Fig. 1).

There is a tendency to parameterize surface GT with a single or a small number of short response times. If outgoing radiation is relatively unresponsive to changes in temperature then $a \to 1$ and $\tau \to \infty$, and Eqn. 2 approximates a random walk, generated by a simple accumulation of heat relative to an equilibrium level forcing S_0.

$$\lim_{a \to 1} T(t) = \frac{1}{C} \sum_{i=0}^{t} (S_i - S_0) \tag{3}$$

More generally, a system composed of several recurrence equations with coefficients $0 < a < 1$ is a Markov chain. It shows long-term memory behavior $f^{-\alpha}$ where $1 < \alpha < 2$ [11]. A large τ will dominate overall system behavior, and given the long response time of the ocean mass, should not be ignored in empirical models.

AR(n) and moving average MA(n) models, where n is the number of lagged terms, are the basis of time series analysis. MA(n) is a finite, moving average model, and can be related to the AR(1) model after n steps with constant forcing S as follows:

$$T_n = a(...(aT_0 + \frac{S}{C})...) + \frac{S}{C} = a^n T_0 + \frac{S}{C} \sum_{t=0}^{n} a^t \tag{4}$$

The summation term of the right hand side approximates a finite n-lag MA(n) exponential filter. When $0 < a < 1$, as $n \to \infty$ then $a^n T_0 \to 0$, and the infinite limit of the geometric series goes to the equilibrium sensitivity $T_s = \tau S/C$. The sum of the finite n coefficients, usually estimated by a statistical MA fitting routine, gives the MA(n) gain.

3 Results

The systems associated with these models can be identified both by statistical test of their characteristics, such Box-Jenkins procedures [12], and also by robust tests. Previous studies confirm that GT data sets normally test as AR(1) or 'red noise' processes [13]. Box-Jenkins procedures [12] on GT datasets show an exponentially declining autocorrelation function (ACF) and partial-ACF that goes to zero at lag=2. By contrast, an MA series shows the opposite ACF and PACF profile. As the input to Eqn. 2 is free, but the response is rate limited, the response to random input should show slower falls than rises, evidenced by an asymmetric distribution of differences. The mean and median of the temperature differences from GT datasets: the EPICA Dome C 800KYr Ice Core [14] data, the surface GT record HadCRUTv3GL [15], and the temperature in the lower troposphere (TLT [16]) are $0.01 > 0.07K$, $0.005 > 0.003K$, $-0.002 > -0.009K$ respectively, consistent with asymmetry and thus output control.

The main characteristic of an accumulation systems is an output proportional to the integral of the input [17]. Thus, output will be more strongly correlated with the cumulative sum of the input than with the input itself. Fig 2 illustrates the direct (red) and accumulated (black) relation to solar irradiance of a range of temperature indices (values listed on Table 1). Satellite-measured atmospheric (TTS, TLT), surface data (HadCRU), ocean heat content (OHC) are plotted against solar irradiance [18]. A millennial temperature proxy (Moberg [19]) is plotted against sun-spot record [20]. The 8000 kYr year EPICA ice-core data are plotted against irradiance from orbital variations in the Southern hemisphere [21]. With the exception of the upper atmosphere (TTS, discussed below), the correlation of accumulated solar irradiance greatly exceeds correlation of the direct relationship. Integrated solar insolation dominates global temperature dynamics over all time scales.

Table 2 lists the estimates of AR parameters for a range of GT datasets by decreasing height: AR is the autocorrelation of the T_i with T_{i+1}, and SD the standard deviation of the residuals. The AR in the troposphere decreases from 0.1 to 0.9 at the surface, corresponding to a response time τ, or system gain from 1 to 10 times the forcing. Two millennial proxy datasets differ at 0.93 [22], and 0.74 [19], while the AR of the 800,000 year EPICA ice-core data is 0.97. The AR of the datasets is linearly related to the log of height (R2=0.98 in the troposphere), indicative of increasing accumulation dynamics with depth, possibly related to the density of the atmosphere (see Fig. 6).

While the previous results illustrate the AR structure of the atmosphere over the short term, we now examine the long-term maximum decay time. The spectral power density of combined GT series over periods spanning 10^6 to 10^{-2} years (Fig. 3) (solid grey line) is inversely related to period $f^{-\alpha}$. The range between $1 < \alpha < 2$ is indicated by lower and upper dashed grey lines respectively. While distortions are a concern, such as attenuation of variance at higher frequencies by averaging and geographic biases, and the Antarctic location of the EPICA record, the result is consistent with the range of stochastic diffusion processes in the coupled atmosphere-ocean system [23].

The $f^{-\alpha}$ spectral scaling shows no clear maximum, indicative of a extremely large τ (or nearly infinite amplification). A possible kickpoint lies between 20ka to 40ka, which by control theory at 2π times the characteristic decay time [17] indicates a τ of at least 3500. Thus for all practical purposes, accumulation dominates the system dynamics. For example, if the standard deviation is 0.1K at the scale of one year, accumulation pre-determines variation over longer periods: 0.23K in 10 years, 0.46K in 100 years, 0.69K in 1000 years and 1.38K over the million years.

The use of MA(0) multiple regressions and MA(n) finite exponential filters on AR(1) systems (e.g. [2]) is questionable not only because a large number of sensitivity λ and lag τ parameters risk overfitting, but also because a finite n-lag MA(n) underestimates the contribution of long-equilibrium effects. We evaluate AR(1) models for potential biases in estimates of the parameters with the use of simulated data. Fig. 4 shows the estimated gain from: MA(0) simple regression, short filter MA(2), long filter MA(10) and AR(1) on simulated AR(1) models at intrinsic gains of 2, 5 and 10 (150 steps, 30 repetitions, a constant forcing of S and random error equal to one). The MA(n) greatly underestimate the known gain, with bias increasing with higher gain because the MA(n) models integrate over shorter time intervals than the equilibration time. The AR(1) model is the least biased. Multiple regression studies are, therefore, miss-specified (e.g. [24]), and studies using a short MA model (e.g. [2]) have seriously underestimated the potential contribution of long-equilibrium forcings.

3.1 Post-1950 Warming

We now fit Eqn. 2 to a number of surface temperature datasets [15, 25] using TSI from [18] as the independent variable (Table 3) over the common years 1882 to 2008. In all cases, the independent TSI term is significant (Pi) and the correlation high (R2). The accumulation of TSI on the HadCRUT3vGL dataset is $0.06 \pm 0.03K/Wm^2/Yr$ when TSI is above or below an equilibrium TSI of $86.2/0.063 = 1365.9Wm^2$ (recovering the solar constant from the empirical data). Thus, the temperature of 159 meters of water would increase by 0.06K after one year at $1W/m^2$, implying that C in the Eqn. 2 has a mass equivalent to the tropical ocean mixed zone over this time-scale. The sensitivity to monthly sunspot number (SS) from the NASA Marshall Flight Center is $0.0001K/SS/Yr$ with an equilibrium of approximately 200 sunspots per annum, and lower correlations.

Accumulated irradiance above equilibrium (CumSolar) to HadCRUT3vGL accounts for 73% (blue) and 76% (red including volcanics) of the variation (Fig. 5). By comparison, the direct TSI has extremely low correlation (orange) (R2=0.024). An additional, compelling finding is zero time lag by cross-correlation of CumSolar with temperature, while temperature lags TSI by one year. The inclusion of a trend term in the regression, such as from increasing GHGs, was not significant (p=0.43 for HadCRUTv3GL and similar for others) and did not improve the model. The confidence interval of the residual trend was $0.0008 \pm 0.0011K/Yr$ indicating with 95% confidence that the limit of detection (LOD) of a residual trend is less than $0.3K$ per century (Table 3 LODs are 0.29, 0.26, 0.26 and 0.12K per century respectively). The solar accumulation model is, therefore, a sufficient explanation for the rise in GT since 1950.

The EBM can be used to distinguish between patterns of warming from enhanced greenhouse effect (EGE) due an increase in the optical density throughout the atmospheric profile, and from natural solar warming ([26] Fig. 9.1). AR and C both increase with decreasing altitude (Fig. 6, triangles, thin black line, extrapolated elevation of 200m). The equilibrium sensitivity $T_s = \tau S/C$ with respect to AR height, a, can be expressed as $Ta(1-a) \propto S$. (The x-axis of Fig. 6 represents units of AR, decadal temperature change and forcing.) With constant forcing implied by EGE and $S = 0.03$, the calculated temperature profile (thick gray dashed line) resembles the mean model projections from [27] (thick gray line), especially the upper troposphere GHG 'hotspot' at 10km or 300mbar.

The altitudinal profile of forcing with a constant temperature change of $T = 0.3$ over the profile (dashed black line) implies a peak forcing in the lower troposphere at 2km, or 800mbar. This largely matches the profile (red band) derived from the mean heights of satellite GT measurements from 1979 (green band) and predicts an increase in mid-troposphere overturning anomaly. Thus, the equilibrium model replicates the climate model outputs under the EGE assumption of a constant forcing over the profile, but peak warming is unrealistically high in the troposphere.

As shown above, uniform temperature rise over the profile agrees better with lower-troposphere trends than uniform forcing. This is realistic for a body in thermal contact, noting also that uniform forcing over the range of AR leads to a singularity at one. The model also predicts a difference in the effectiveness of solar and GHG forcings. A forcing weighted exerted towards the lower AR=1 level of the profile, such as solar radiation, will have higher gain (and so larger effects on temperature) than an atmospheric forcing in the higher levels of the profile, such as GHGs, where AR<1.

3.2 Climate Sensitivity

Let us interpret the estimation climate sensitivity in light of the accumulation model. If we let the heat flux at the top of atmosphere (TOA) be an independent random variable (i.e. AR=0), the temperature series are progressively decorrelated down through the atmospheric profile, due to the statistics of the accumulation process. The (almost) random walk at the bottom (AR=0.9) would be almost uncorrelated with the TOA. Determinations of climate sensitivity by correlation of TOA (y axis) with the change in global temperature (x axis) are, therefore, questionable [28, 29]. For example, Fig 7 is a scatter plot of a simulated AR(1)=0 series and its AR(1) accumulant at AR=0.5 (mid-troposphere) and AR=0.9 (surface). The trend at AR=0.5 is steep, and the trend at AR=0.9 is low, supposedly indicative of low and high sensitivity respectively. Furthermore, the high AR on Fig 7 shows striation and spiral patterns indicative of 'non-forced decadal variability' [28]. However, these phenomena are simply artifacts of the autocorrelation structure of the system, and unrelated to intrinsic sensitivity.

As follows from thermal conductivity, a sustained temperature change at any level will eventually be equilibrated throughout the lapse rate, the surface and deep ocean. The relative effect of a distributed forcing can be determined by integrating the $T(a - a^2) = S$ over the atmospheric profile. Thus, a one degree change at the surface where AR=0.9 would require a forcing of one eleventh, while a forcing distributed evenly through the atmosphere, like a GHG, would be one sixth, i.e.:

$$\int (a - a^2) da = [\frac{a^2}{2} - \frac{a^3}{3}]_0^1 = \frac{1}{6}$$

If these assumptions resemble the distribution of solar and GHG forcings, they would explain, to a first approximation, high solar sensitivity with low GHG sensitivity. However, the dominant response of the system is determined not only by the autocorrelation AR, but also by the attenuation of heat into the high AR, oceanic, accumulators [30, 10].

4 Discussion

An appropriate physics-based model is essential for designing and interpreting empirical analysis. The dynamics generated by an integration process in which the output is proportion to the integration of the input, lead to quite different results from a directly proportional process. Most importantly, accumulation is a mechanism for the apparent high sensitivity of GT to solar variations.

The objections that by direct correlation the amplitude of the 11 year solar cycle is no more than a few hundredths of a degree [31], the trend in TSI since 1950 has been small [32], and in the wrong direction since the Grand Solar Maximum in 1986 [33], incorrectly assume a fast and direct solar influence. Inadequate short-exponential MA filters bias downward the contribution of the slow-equilibrium process. Such methods greatly underestimate the contribution of slow, accumulated forcings from the Sun.

Most of the variation and rise of GT since 1950, with the correct phase of the solar cycle, can be explained by the gain or loss of $0.06 \pm 0.03C/Wm^2/Yr$ when TSI differs from the equilibrium solar constant of $S_0 = 1365.9Wm^2$. These results are consistent with phenomenological analysis attributing of over half the GT change since the 1970's to natural climate oscillations [1] and the flat warming/cooling rate of $0.1 \pm 0.2W/m^2$ ocean heat content anomaly since 2003 [3] (Fig. 5). As is well known, solar activity during the past 70 years is exceptional for at least 8,000 years [20] and this study describes the mechanism whereby this activity could produce the strong warming observed during the past three decades.

Net anthropogenic forcings may confound the determination of the equilibrium level S_0 for post 1950 warming, and consequently the relative solar contribution to recent warming is quite uncertain. This uncertainty does not arise over longer time scales where the S_0 may be taken as the mean over the period. Many observations are explained by the accumulative model, such as higher correlation of integrated solar intensity over six orders of time, the $f^{-\alpha}$ spectral response of temperature over paleoclimatic timescales, asymmetric differences, the statistical characteristics of atmospheric time-series, the agreement with the atmospheric profile of warming, and many more.

The conventional statement (H_0) that changes in GHG concentrations explain the majority of recent and paleoclimatic variability [34] stands in opposition to the alternative (H_a) that GT dynamics are indistinguishable from accumulation of solar heat, with changes in GHGs and surface albedo maintaining the AR structure of the atmosphere. Note that the H_a does not exclude the possibility of observable effects from rising GHG concentrations, whereas H_0 excludes the possibility of distinct solar effects. Exotic solar effects on climate such as solar modulated galactic cosmic (gamma) ray fluxes and clouds [35] affect the magnitude of solar forcing, and not the accumulation dynamics.

Climate models explain recent warming in terms of GHG increases, but suffer from a number of limitations that mitigate against interpreting the match of model with observations as proof of dominance by GHGs. They are known to underestimate the observed response to solar forcing [36], and poor parametrisation of ocean mixing parameters exaggerates warming from GHGs [4], as energy flows across the thermocline [30] are up to 50 times less than used in climate models [30, 10]. We have simulated an upper troposphere 'hotspot' seen in the climate model projections, but not yet observed [27, 5], with a constant forcing assumption due to increased optical depth of GHGs. The opacity of CO_2 by spectral studies of the upper atmosphere and fingerprint attribution studies are also subject to large uncertainties [37] and confounding influences, ie. ozone depletion also cools the upper stratosphere.

5 Acknowledgements

In working at the problem here I have had the loyal assistance of my friend and colleague Anthony Cox, and I am indebted to Demetris Koutsoyiannis, Geoffery Sherrington and David Hagen reviews of preliminary drafts.

References

[1] Nicola Scafetta. Empirical analysis of the solar contribution to global mean air surface temperature change. *Journal of Atmospheric and Solar-Terrestrial Physics*, 71(17-18):1916–1923, December 2009.

[2] M. Lockwood. Solar change and climate: an update in the light of the current exceptional solar minimum. *Proceedings of the Royal Society A: Mathematical, Physical and Engineering Sciences*, 466(2114):303–329, December 2009.

[3] R S Knox and D H Douglass. Recent energy balance of Earth. *Online*, 1(3):2–4, 2010.

[4] James Hansen, Makiko Sato, Pushker Kharecha, and Karina von Schuckmann. Earth's Energy Imbalance and Implications. *eprint arXiv:1105.1140*, page 52, May 2011.

[5] Ross McKitrick, Stephen McIntyre, and Chad Herman. Panel and multivariate methods for tests of trend equivalence in climate data series. *Atmospheric Science Letters*, 11(4):270–277, October 2010.

[6] Qiang Fu, Syukuro Manabe, and Celeste M. Johanson. On the warming in the tropical upper troposphere: Models versus observations. *Geophysical Research Letters*, 38(15):L15704, August 2011.

[7] Mike Lockwood and Claus Fröhlich. Recent oppositely directed trends in solar climate forcings and the global mean surface air temperature. II. Different reconstructions of the total solar irradiance variation and dependence on response time scale. *Proceedings of the Royal Society A: Mathematical, Physical and Engineering Sciences*, 464(2094):1367–1385, June 2008.

[8] J Lean and D Rind. Sun-climate connections. Earth's response to a variable Sun. *Science*, 292(5515), 2001.

[9] R Muscheler, F Joos, J Beer, S Muller, M Vonmoos, and I Snowball. Solar activity during the last 1000yr inferred from radionuclide records. *Quaternary Science Reviews*, 26(1-2):82–97, January 2007.

[10] D. H. Douglass, R. S. Knox, B. D. Pearson, and a. Clark. Thermocline flux exchange during the Pinatubo event. *Geophysical Research Letters*, 33(19):1–5, October 2006.

[11] Sveinung Erland and Priscilla Greenwood. Constructing 1âĹŢω^{α} noise from reversible Markov chains. *Physical Review E*, 76(3):031114, September 2007.

[12] George Box, Gwilym Jenkins, and Gregory Reinsel. *Time Series Analysis: Forecasting & Control (3rd Edition)*. Prentice Hall, 3rd edition, 1994.

[13] Xiaogu Zheng, Reid E. Basher, and Craig S. Thompson. Trend Detection in Regional-Mean Temperature Series: Maximum, Minimum, Mean, Diurnal Range, and SST. *Journal of Climate*, 10(2):317–326, February 1997.

[14] J Jouzel, V Masson-Delmotte, O Cattani, G Dreyfus, S Falourd, G Hoffmann, B Minster, J Nouet, J M Barnola, J Chappellaz, H Fischer, J C Gallet, S Johnsen, M Leuenberger, L Loulergue, D Luethi, H Oerter, F Parrenin, G Raisbeck, D Raynaud, A Schilt, J Schwander, E Selmo, R Souchez, R Spahni, B Stauffer, J P Steffensen, B Stenni, T F Stocker, J L Tison, M Werner, and E W Wolff. Orbital and millennial Antarctic climate variability over the past 800,000 years. *Science (New York, N.Y.)*, 317(5839):793–6, August 2007.

[15] P D Jones, M New, D E Parker, S Martin, and I G Rigor. Surface air temperature and its variations over the last 150 years. *Reviews of Geophysics*, 37:137–199, 1999.

[16] Carl A. Mears and Frank J. Wentz. Construction of the RSS V3.2 Lower-Tropospheric Temperature Dataset from the MSU and AMSU Microwave Sounders. *Journal of Atmospheric and Oceanic Technology*, 26(8):1493–1509, August 2009.

[17] Allen Stubberud, Ivan Williams, and Joseph DiStefano. *Schaum's Outline of Feedback and Control Systems (Schaum's)*. McGraw-Hill, 1994.

[18] J. L. Lean. Solar irradiance and climate forcing in the near future. *Geophysical Research Letters*, 28(21):4119, 2001.

[19] Anders Moberg, Dmitry M Sonechkin, Karin Holmgren, Nina M Datsenko, and Wibjorn Karlen. Highly variable Northern Hemisphere temperatures reconstructed from low- and high-resolution proxy data. *Nature*, 433(7026):613–617, 2005.

[20] S K Solanki, I G Usoskin, B Kromer, M Schüssler, and J Beer. Unusual activity of the Sun during recent decades compared to the previous 11,000 years. *Nature*, 431(7012):1084–7, October 2004.

[21] A. Berger and M.F. Loutre. Insolation values for the climate of the last 10 million years. *Quaternary Science Reviews*, 10(4):297–317, January 1991.

[22] C Loehle. A 2000-year global temperature reconstruction based on non-treering proxies. *Energy & Environment*, 19(1):93–100, 2007.

[23] Jon D Pelletier. Natural variability of atmospheric temperatures and geomagnetic intensity over a wide range of time scales. *Proceedings of the National Academy of Sciences of the United States of America*, 99 Suppl 1(90001):2546–53, February 2002.

[24] Gabriele C. Hegerl. Detection of volcanic, solar and greenhouse gas signals in paleo-reconstructions of Northern Hemispheric temperature. *Geophysical Research Letters*, 30(5):46–1, 2003.

[25] James Hansen and Sergej Lebedeff. Global Trends of Measured Surface Air Temperature. *Journal of Geophysical Research*, 92(D11):13345–13372, 1987.

[26] IPCC. *Climate Change 2007: The Physical Science Basis. Contribution of Working Group I to the Fourth Assessment Report of the Intergovernmental Panel on Climate Change*. Cambridge University Press 32 Avenue of the Americas, New York, NY 10013-2473, USA, 2007.

[27] B. D. Santer, P. W. Thorne, L. Haimberger, K. E. Taylor, T. M. L. Wigley, J. R. Lanzante, S. Solomon, M. Free, P. J. Gleckler, P. D. Jones, T. R. Karl, S. A. Klein, C. Mears, D. Nychka, G. A. Schmidt, S. C. Sherwood, and F. J. Wentz. Consistency of modelled and observed temperature trends in the tropical troposphere. *International Journal of Climatology*, 28(13):1703–1722, November 2008.

[28] Roy W Spencer and William D Braswell. On the diagnosis of radiative feedback in the presence of unknown radiative forcing. *J. Geophys. Res.*, 115(D16), 2010.

[29] A E Dessler. A determination of the cloud feedback from climate variations over the past decade. *Science (New York, N.Y.)*, 330(6010):1523–7, December 2010.

[30] T. M. L. Wigley. Comment on âĂIJClimate forcing by the volcanic eruption of Mount PinatuboâĂİ by David H. Douglass and Robert S. Knox. *Geophysical Research Letters*, 32(20):L20709, October 2005.

[31] G. R. North, Q. Wu, and M. J. Stevens. Detecting the 11-year Solar Cycle in the Surface Temperature Field. *Solar Variability and its Effects on Climate. Geophysical Monograph 141*, 2004.

[32] P Foukal, C Fröhlich, H Spruit, and T M L Wigley. Variations in solar luminosity and their effect on the Earth's climate. *Nature*, 443(7108):161–6, September 2006.

[33] M. Lockwood, A. P. Rouillard, and I. D. Finch. The rise and fall of open solar flux dueing the current grand solar maximum. *The Astrophysical Journal*, 700(2):937–944, August 2009.

[34] Phillip B. Duffy, Benjamin D. Santer, and Tom M.L. Wigley. Solar variability does not explain late-20th-century warming. *Physics Today*, 62(1), 2009.

[35] Henrik Svensmark. Cosmoclimatology: a new theory emerges. *Astronomy & Geophysics*, 48(1):1.18–1.24, February 2007.

[36] Peter a. Stott, Gareth S. Jones, and John F. B. Mitchell. Do Models Underestimate the Solar Contribution to Recent Climate Change? *Journal of Climate*, 16(24):4079, 2003.

[37] Q.B. Lu. What is the Major Culprit for Global Warming: CFCs or CO2? *Journal of Cosmology*, 8:1846–1862, 2010.

6 Figures

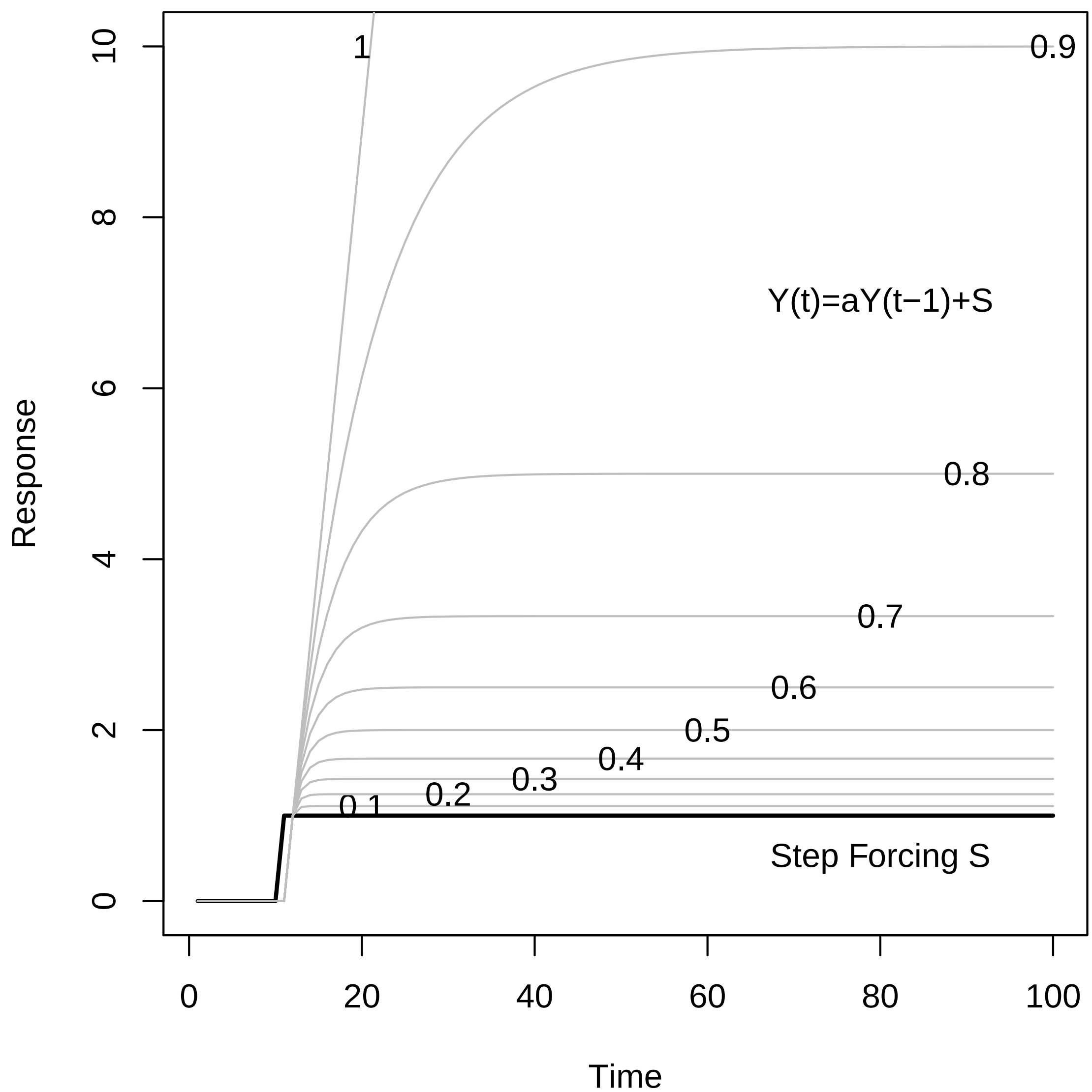

Figure 1: Response of an AR(1) model to a step forcing S (black) for a range of coefficients (gray).

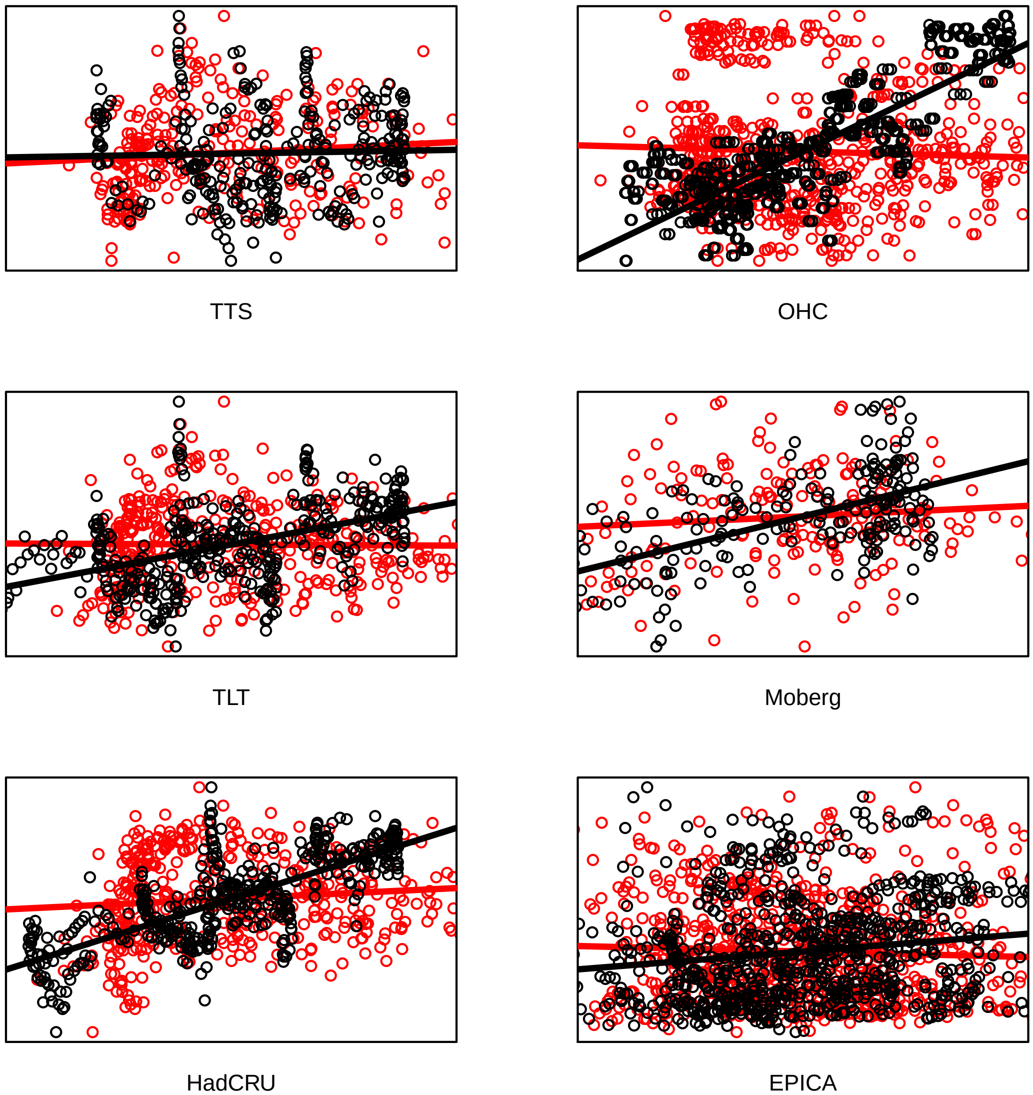

Figure 2: Direct correlation of global temperature (red) and the cumulative sum (black) with solar insolation from the annual to million year time scales.

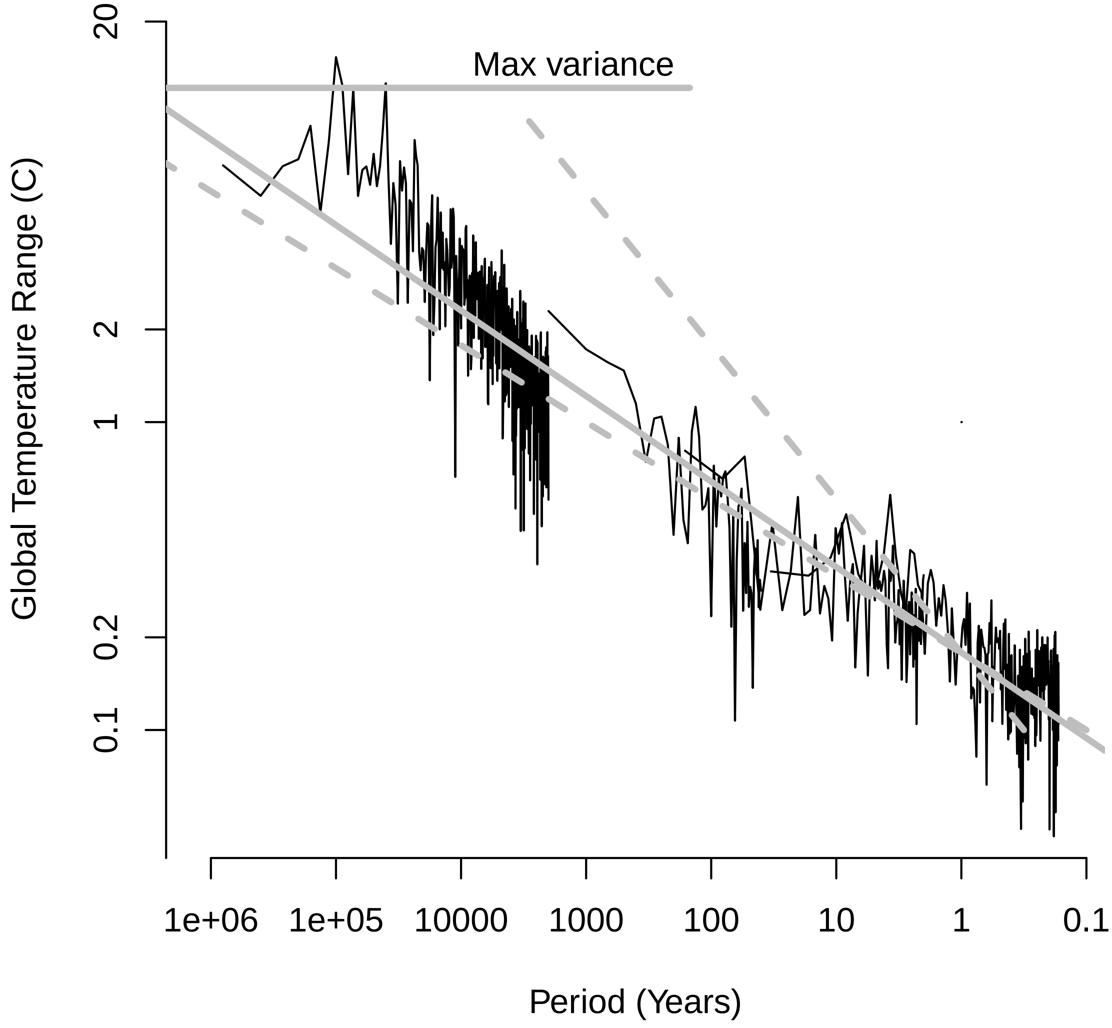

Figure 3: Power density spectrum of GT datasets over 1Ma (fit is solid grey line) and the f^{-1} (lower dashed) and f^{-2} (upper dashed) lines, and a possible maximum amplitude at 40,000 years.

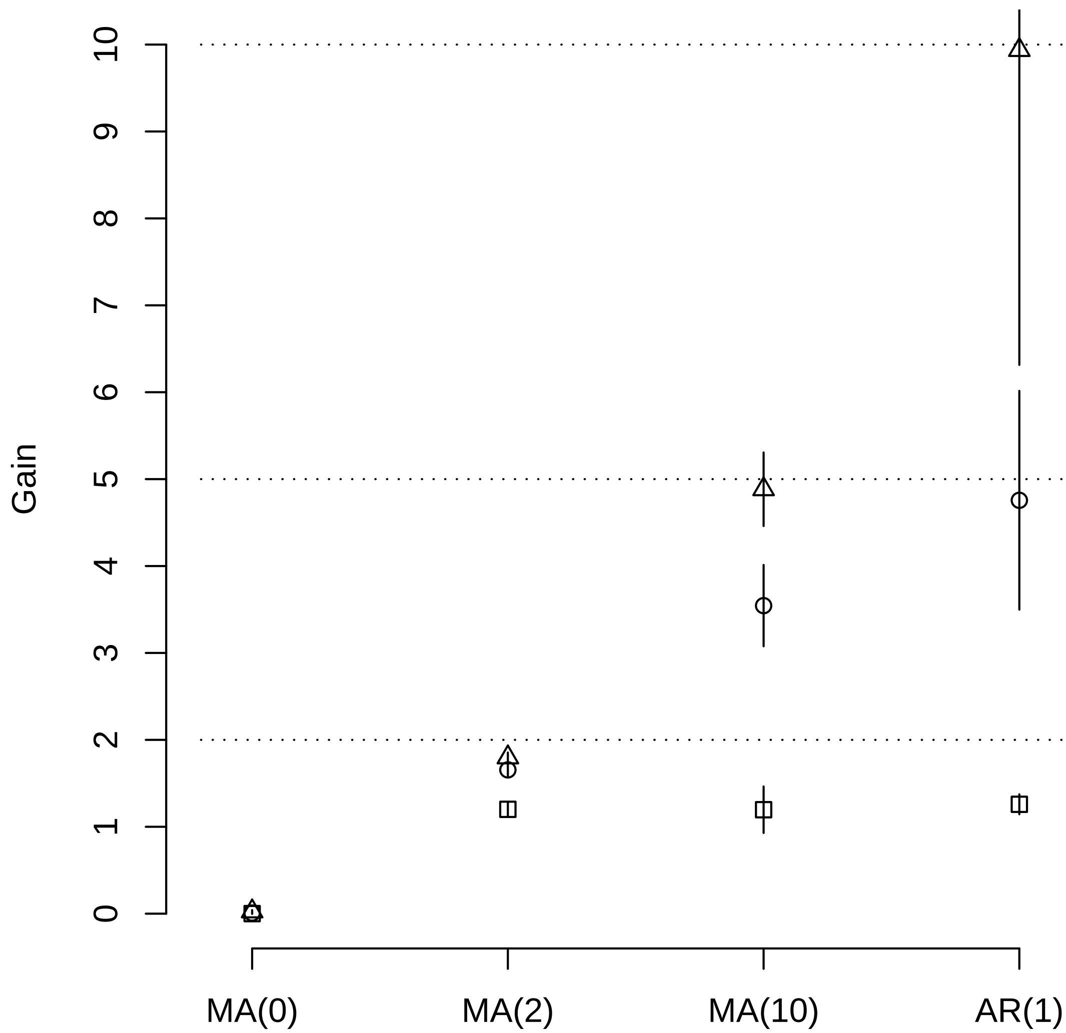

Figure 4: The recovery of known gains by models. AR(1) model with gains of 2 (squares), 5 (circles), and 10 (triangles) by simple regression MA(0), short exponential MA(2), long exponential MA(10), and an AR(1) model.

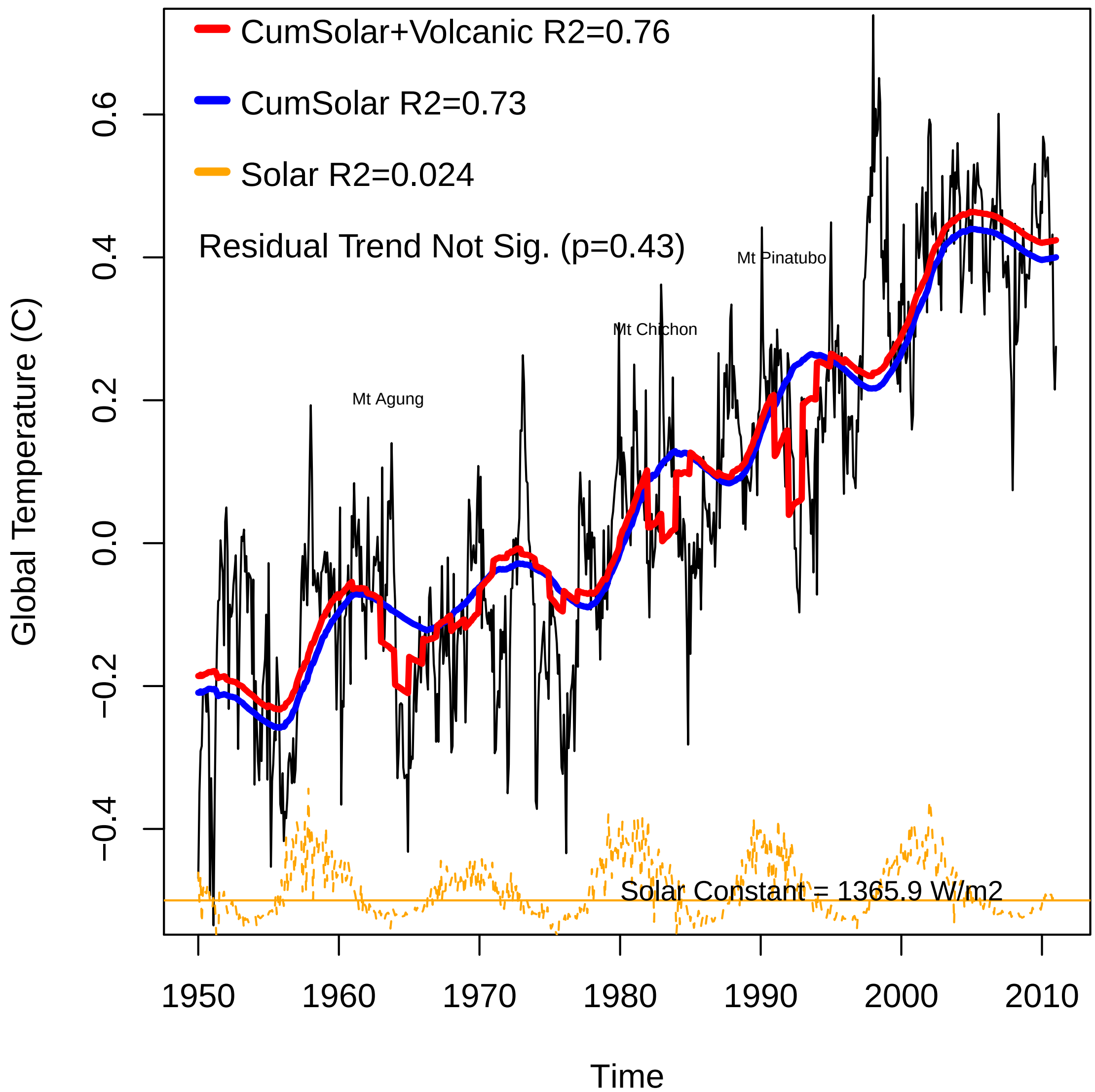

Figure 5: Regression of HadCRUTv3GL with solar intensity (blue) and (red) volcanic forcing. The solar irradiance and solar constant (orange) is on the lower axis.

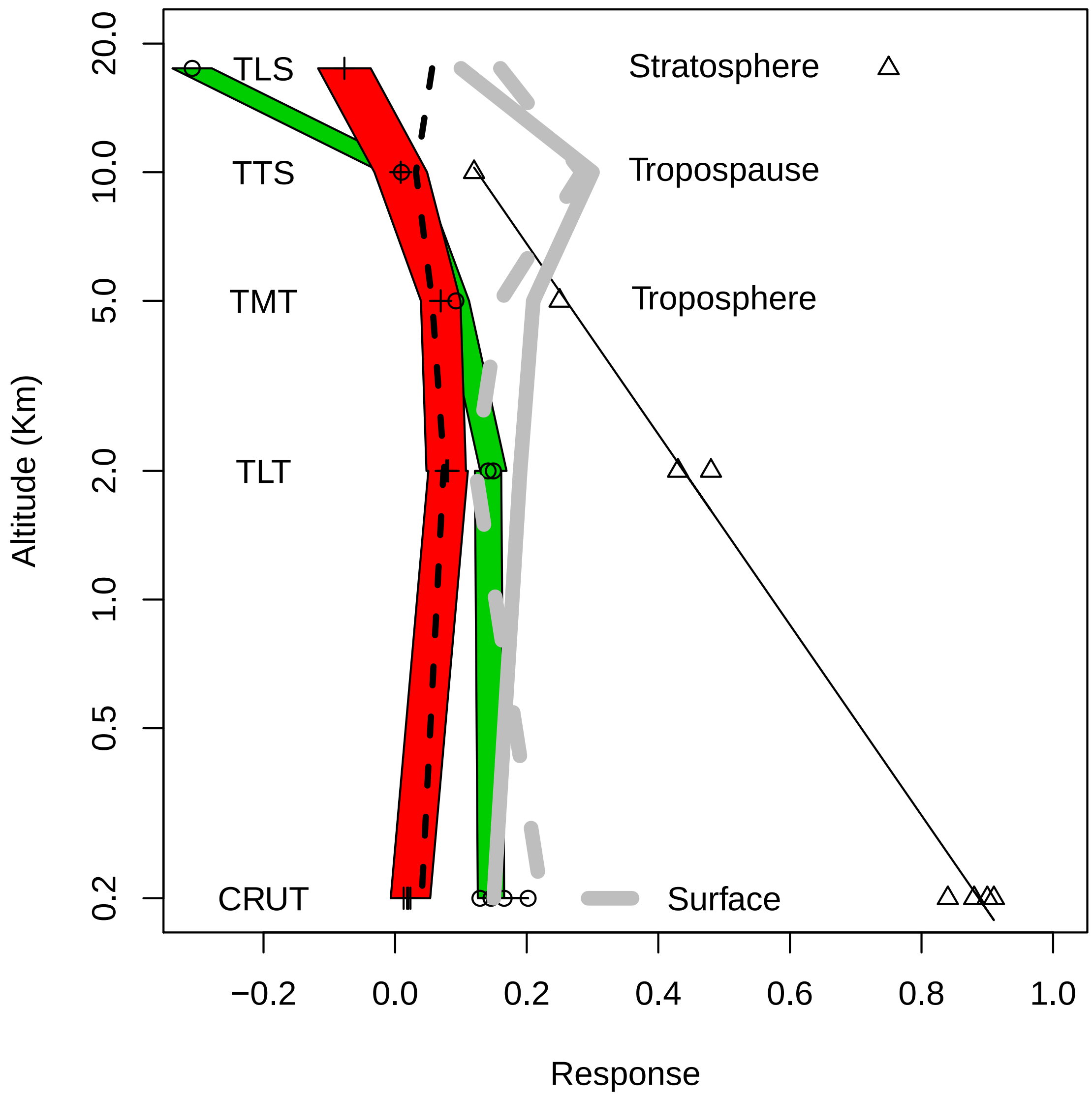

Figure 6: Application of equilibrium relationship between temperature and forcing over atmospheric profile. The AR (x-axis) varies linearly with the log of altitude (triangles, thin black line). Calculated temperature change (in K/decade on x-axis) over the profile assuming constant forcing (thick gray dashed line) agrees with mean climate model projections from [27] (thick gray line). Forcing over height (in W/m2 also on x-axis) (red band) implied by observed satellite warming trends from 1979 (green band) agrees with calculated forcing assuming constant temperature change over the profile (dashed black line).

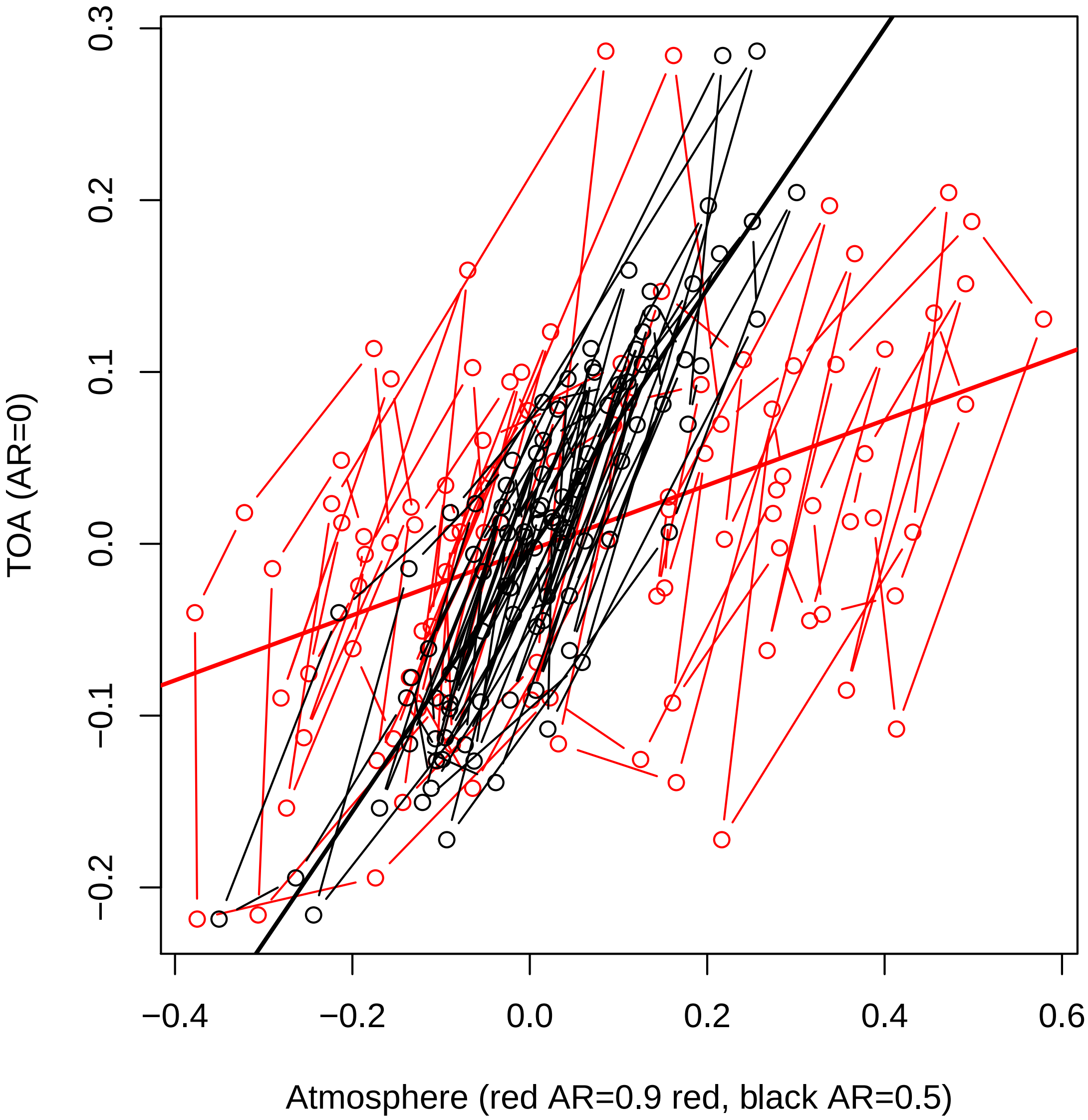

Figure 7: The correlation of a random (AR(1)=0) series with its accumulants at AR=0.5 (mid-troposphere) and AR=0.9 (surface). The trend is indicative or relative position in the profile, and not the inherent the climate sensitivity.

7 Tables

	R2 Direct	R2 Integ
TTS	0.01	0.00
TLT	0.00	0.23
HadCRU	0.01	0.56
OHC	0.00	0.69
Moberg	0.01	0.30
EPICA	0.00	0.03

Table 1: Direct correlation of temperature indices with solar insolation (R2 Direct) and with the cumulative sum of the insolation anomaly (R2 Integ).

	Km	AR	sd1	SD	Tau
UAH	18	0.43	0.16	0.18	1.7
TLT	10	0.48	0.16	0.18	1.9
TMT	5	0.25	0.18	0.16	1.3
TTS	2	0.12	0.21	0.17	1.1
TLS	2	0.75	0.12	0.27	3.9
HadCRU	0	0.91	0.03	0.11	11.3
HadSST	0	0.90	0.03	0.11	9.8
HadLST	0	0.84	0.04	0.17	6.4
GISS	0	0.88	0.04	0.11	8.7
loehle		0.93	0.04	0.09	14.1
moberg		0.74	0.07	0.12	3.9
vosreg		0.97	0.01	0.75	29.3

Table 2: Estimates of the AR coefficients and standard deviation of residuals (SD) for a range of GT datasets.

	C/Wm2/Yr	Tau	W/m2	R2	Pi
HadCRU	0.0527	10.8	1366.0	0.87	0.06
HadSST	0.0571	8.1	1366.1	0.84	0.05
HadLST	0.0836	7.1	1365.9	0.79	0.06
GISS	0.0589	6.9	1365.8	0.81	0.07

Table 3: Parameter estimates of the regression (Eqn 2) from annual GT with Lean et.al. 2001 annual solar irradiance data: K/Wm2/Yr - climate sensitivity, Tau - intrinsic gain, W/m2 - the derived solar constant, R2 is the correlation coefficient and Pi the p-value of the independent variable, annual solar irradiance.